ISSN 0915-633X

NATIONAL INSTITUTE FOR FUSION SCIENCE

A New Algorithm for Differential-Algebraic Equations Based on HIDM

T. Watanbe, G. Gnudi

(Received - Feb. 13, 1995)

NIFS-341 Feb. 1995

RESEARCH REPORT
NIFS Series

NAGOYA, JAPAN

A NEW ALGORITHM FOR DIFFERENTIAL-ALGEBRAIC EQUATIONS BASED ON HIDM

WATANABE Tsuguhiro
National Institute for Fusion Science
Chikusaku, Nagoya, 464-01, Japan
E-mail: wata@simsun.nifs.ac.jp

Giovanni GNUDI
National Institute for Fusion Science
Chikusaku, Nagoya, 464-01, Japan
E-mail: gnudi@srhatori.nifs.ac.jp

ABSTRACT

A new algorithm is proposed to solve differential-algebraic equations. The algorithm is an extension of the algorithm of general purpose **HIDM** (higher order implicit difference method). A computer program named **HDMTDV** and based on the new algorithm is constructed and its high performance is proved numerically through several numerical computations, including index-2 problem of differential-algebraic equations and connected rigid pendulum equations.
The new algorithm is also secular error free when applied to dissipationless dynamical systems. This nature is demonstrated numerically by computation of the Kepler motion. The new code can solve the initial value problem

$$\mathbf{0} = \boldsymbol{L}\left(\varphi(x), \frac{d\,\varphi(x)}{d\,x}, \frac{d^2\,\varphi(x)}{d\,x^2}, x\right) ,$$

where $\boldsymbol{L}$ and φ are vectors of length N. The values of first or second derivatives of $\varphi(x)$ are not always necessary in the equations.

1. Introduction

Computer analysis is playing more and more important roles for the development of science and technology. High speed and large scale computers together with powerful algorithms are extending the field of activity of numerical computations. Many types of equations are waiting to be solved numerically in the course of research and development.

There are many excellent algorithms to solve the initial value problems described by non-stiff ordinary differential equations. We can usually get good solutions for such problems by excellent ready-made computer programs. However, we encounter sometimes serious numerical difficulties if the problems are reduced to stiff ordinary differential equations, or to differential-algebraic equations. Differential-algebraic equa-

Keywords: **HIDM**, differential-algebraic equations, stiff differential equations, symplectic integrator, time reversal integrator

tions frequently arise in many physical problems, such as optimal control problems, dynamical systems with constrained conditions and so on. The present status of the research on differential-algebraic equations is described in references[1,2,3].

In a previous paper[4] we have constructed a new computer program named **HIDMDV** (HIDM with second derivative) to solve stiff ordinary differential equations or differential-algebraic equations, based on the algorithm **HIDM** (higher order implicit difference method)[5,6,7,8]. The program **HIDMDV** can solve the equation

$$\mathbf{0} = \boldsymbol{L}\Big(\boldsymbol{\varphi}(x),\ \boldsymbol{\varphi}'(x),\ \boldsymbol{\varphi}''(x),\ x\Big), \tag{1}$$

where $\boldsymbol{L}$ and $\boldsymbol{\varphi}$ are vectors of length N. To solve Eq.(1), we have introduced the difference scheme as shown in Fig.1.

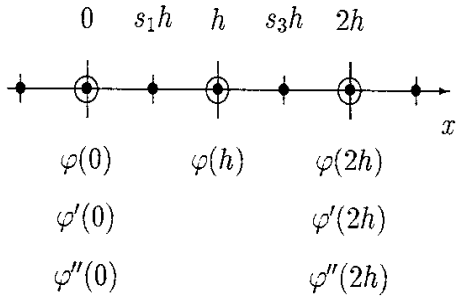

Fig.1 The difference scheme for **HIDMDV**. The values $\varphi(0)$ and $\varphi'(0)$ are given as initial values for rank-2 ordinary differential equations. The remaining 5 function values at grid points shown by ○ (equally separated points) are obtained numerically, by solving the differential equations at 5 intermediated points shown by • (unequally separated points). The values $s_i (i = 1, 3)$ are uniquely determined from the minimization of the truncation error for $\varphi''(s_i h)$.

The computer program **HIDMDV** has shown good performance and has been extended to be able to solve boundary-value and eigenvalue problems[4]. However, practical applications has revealed that the algorithm of **HIDMDV** should be improved from the point of view of accuracy and easiness of use.

The algorithm of **HIDMDV** is proved to be A-Stable but not secular error free for dissipationless dynamical systems. For long time tracing of dynamical systems, symplectic integrators[9,11,10,12] have attracted considerable attention because they are free from secular errors. Recently, Watanabe and Gnudi[13] has extended the algorithm **HIDMDV** to satisfy the no secular error property by introducing the idea of time-reversal integrator.

The computer program **HIDMDV** is designed to solve the second derivative $\varphi''(x)$ at the grid points (see Fig.1). Additional equations are needed if the Eq.(1)

contains no second derivatives $\varphi''(x)$. This requirement makes the use of **HIDMDV** occasionally complicated in applications.

In this paper, we have extended the algorithm of **HIDMDV** in order to satisfy the time reversibility and to have a more easy-to-use nature. A computer program named **HDMTDV** (HIDM, time reversal with second derivative) is constructed based on this new algorithm.

In section **2** we summarize the principle of the **HDMTDV**. Numerical examples of **HDMTDV** are shown in section **3**. Section **4** is devoted to a short summary.

2. Principle of HDMTDV

The principle of **HIDM** is shown in detail in references[5,6,7]. Here we summarize the principle of **HDMTDV**, which can solve differential-algebraic equations without the trouble accompanying non adaptive initial conditions. Furthermore, **HDMTDV** has a linearly symplectic nature, and guarantees absence of secular errors for recursive motions of dissipationless dynamical systems. There are 3 types of **HDMTDV** difference scheme, depending on the highest derivatives of each variable. These are discussed in the following subsections.

2.1. Difference Scheme for Variables with Second Derivative

Here, we consider the difference scheme for variables which have second derivatives in Eq.(1). In this case, we use the difference scheme shown in Fig.2.

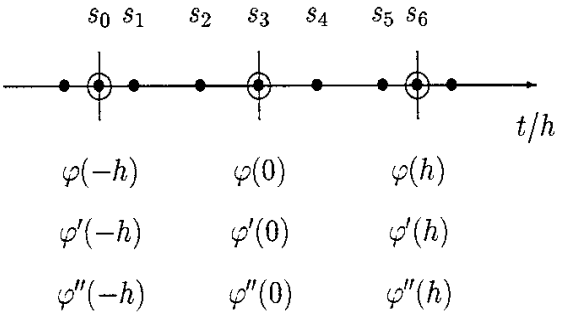

Fig.2 The difference scheme for variables having second derivatives in Eq.(1). The values $\varphi(-h)$ and $\varphi'(-h)$ are given as initial values for rank-2 ordinary differential equations. The remaining 7 function values at grid points shown by ○ (equally separated points) are obtained numerically, by solving the differential equations at 7 intermediated points, shown by • (unequally separated points). The values $s_i (i = 1, 2, 4, 5)$ are uniquely determined from the condition that truncation error for $\varphi''(s_i h)$ should be minimized ($s_0 = -1$, $s_3 = 0$, $s_6 = 1$).

Expressions of the function and its derivatives at the points $x = s_i h$ $(i = 0, \cdots, 6)$

are given by linear combinations of function values at grid points $x = -h,\ 0,\ h$ as follows

$$\varphi''(sh) = \frac{1}{h^2}\sum_{j=-1}^{1} P_j(s)\varphi(jh) + \frac{1}{h}\sum_{j=-1}^{1} Q_j(s)\varphi'(jh) + \sum_{j=-1}^{1} R_j(s)\varphi''(jh)\,, \quad (2)$$

$$\varphi'(sh) = \frac{1}{h}\sum_{j=-1}^{1} D_j(s)\varphi(jh) + \sum_{j=-1}^{1} E_j(s)\varphi'(jh) + h\sum_{j=-1}^{1} F_j(s)\varphi''(jh)\,, \quad (3)$$

$$\varphi(sh) = \sum_{j=-1}^{1} A_j(s)\varphi(jh) + h\sum_{j=-1}^{1} B_j(s)\varphi'(jh) + h^2\sum_{j=-1}^{1} C_j(s)\varphi''(jh)\,. \quad (4)$$

The difference scheme for the second derivative φ'', Eq.(2), has a total of 9 parameters $(P_j(s),\ Q_j(s),\ R_j(s))$. Then the truncation error for Eq.(2) becomes $O(h^7)$. To reduce this truncation error we introduce a relation which determines the value of s as follows

$$1 - 9s^2 + 12s^4 = 0\,, \quad (5)$$

that is

$$s_1 = -0.7838\cdots\,,\ s_2 = -0.3682\cdots\,,\ s_4 = 0.3682\cdots\,,\ s_5 = 0.7838\cdots\,. \quad (6)$$

Then the values of $(P_j(s_i),\ Q_j(s_i),\ R_j(s_i))$, $(j = -1, 0, 1,\ i = 0, \cdots, 6)$ are determined uniquely, and then truncation error of Eq.(2) becomes $O(h^8)$.

The difference scheme for φ', Eq.(3) has a total of 9 parameters $(D_j(s),\ E_j(s),\ F_j(s))$. Then the truncation errors for Eq.(3) becomes $O(h^8)$. This order is compatible with the one of Eq.(2). Then, the parameters $(D_j(s),\ E_j(s),\ F_j(s))$ are also determined uniquely.

The difference scheme for φ, Eq.(4), has a total of 9 parameters $(A_j(s),\ B_j(s),\ C_j(s))$. Then the truncation errors for Eq.(4) can be reduced to $O(h^9)$. This order is one order higher than the one of Eq.(2) and Eq.(3). Then one parameters, for example $C_1(s)$, becomes free if we are satisfied with the same order of accuracy of the discretization scheme for φ, φ', φ''. When we impose the time reversal condition for the discretization scheme Eqs.(2–4), we obtain the conditions

$$C_1(s_2) - C_1(s_4) = -\frac{111 + \sqrt{33}}{9216}s_4\,. \quad (7)$$

$$C_1(s_1) - C_1(s_5) = -\frac{111 - \sqrt{33}}{9216}s_5\,. \quad (8)$$

Two coefficients are still left undetermined for the parameters $(A_j(s_i),\ B_j(s_i),\ C_j(s_i))$, $(j = -1, 0.1,\ i = 0, \cdots, 6)$, if we request the compatibility for the truncation errors for representations Eqs.(2–3). We discuss about this points in some detail in the section 4.

In the following, we determine the parameters in Eq.(4) in order to minimize the truncation error for $\varphi(s)$. In this case the truncation error of Eq.(4) becomes $O(h^9)$, which is one order higher than the one of φ' and φ''. Coefficients for the discretization scheme of **HDMTDV** are reduced to the form

$$A_{\pm 1}(s) = \frac{4278 + 598\Delta \pm (7569 + 513\Delta)s}{36864}, \quad A_0(s) = \frac{2469 - 299\Delta}{4608}, \tag{9}$$

$$B_{\pm 1}(s) = \frac{\mp(2937 + 361\Delta) - (6372 + 164\Delta)s}{73728}, \quad B_0(s) = \frac{(405 - 59\Delta)s}{1152}, \tag{10}$$

$$C_{\pm 1}(s) = \frac{161 + 17\Delta \pm (444 - 4\Delta)s}{73728}, \quad C_0(s) = \frac{283 - 21\Delta}{3072}, \tag{11}$$

$$D_{\pm 1}(s) = \frac{(111 - \Delta)(\pm 35 + 64s)}{6144}, \quad D_0(s) = -\frac{(111 - \Delta)s}{48}, \tag{12}$$

$$E_{\pm 1}(s) = -\frac{351 - 529\Delta \pm (2088 - 600\Delta)s}{18432}, \quad E_0(s) = -\frac{261 + 53\Delta}{1152}, \tag{13}$$

$$F_{\pm 1}(s) = \frac{\mp(39 + 55\Delta) + (72 - 56\Delta)s}{18432}, \quad F_0(s) = -\frac{(9 - 7\Delta)s}{144}, \tag{14}$$

$$P_{\pm 1}(s) = -\frac{312 + 440\Delta \mp (945 - 735\Delta)s}{768}, \quad P_0(s) = \frac{35 + 55\Delta}{48}, \tag{15}$$

$$Q_{\pm 1}(s) = \frac{\pm(209 + 65\Delta) + (173 + 93\Delta)s}{256}, \quad Q_0(s) = -\frac{(61 - 19\Delta)s}{16}, \tag{16}$$

$$R_{\pm 1}(s) = -\frac{117 + 37\Delta \pm (99 + 51\Delta)s}{2304}, \quad R_0(s) = -\frac{9 - 7\Delta}{16}, \tag{17}$$

where

$$\Delta = \begin{cases} \sqrt{33} & (\text{ for } s = s_1 \text{ or } s_5)\,, \\ -\sqrt{33} & (\text{ for } s = s_2 \text{ or } s_4)\,. \end{cases} \tag{18}$$

Time reversibility conditions given by

$$A_j(s_i) = A_{-j}(s_{6-i}), \quad B_j(s_i) = -B_{-j}(s_{6-i}), \quad C_j(s_i) = C_{-j}(s_{6-i})\,, \tag{19}$$

$$D_j(s_i) = -D_{-j}(s_{6-i}), \quad E_j(s_i) = E_{-j}(s_{6-i}), \quad F_j(s_i) = -F_{-j}(s_{6-i})\,, \tag{20}$$

$$P_j(s_i) = P_{-j}(s_{6-i}), \quad Q_j(s_i) = -Q_{-j}(s_{6-i}), \quad R_j(s_i) = R_{-j}(s_{6-i})\,, \tag{21}$$

$$(j = -1, 0, 1), \quad (i = 1, 2, 4, 5)$$

are completely satisfied.

Next we consider the stability of the discretization scheme given by Eq.(9–17) by solving the characteristic frequency of the harmonic oscillator

$$\varphi''(x) + \omega^2 \varphi(x) = 0\,, \tag{22}$$

where ω is some constant. If we express the eigenfunction of Eq.(22) under the discretization scheme by

$$\varphi(nh) \propto \exp(i\, nh\Omega)\,, \tag{23}$$

we get the dispersion relation

$$\cos(2h\Omega) = \frac{457228800 - 881118000g + 239415750g^2 - 20934585g^3 + 724410g^4 - 9792g^5 + 38g^6}{457228800 + 33339600g + 1275750g^2 + 33075g^3 + 540g^4 - 18g^5 + 2g^6}\,, \tag{24}$$

where $g \equiv (h\omega)^2$.

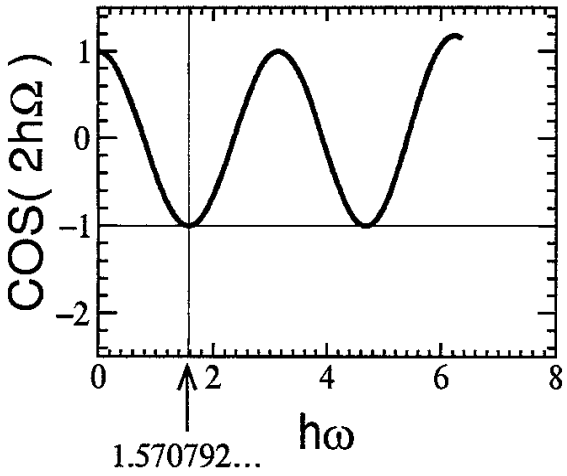

Fig.3 The dispersion curve of the harmonic oscillator given by Eq.(22) under the discretization scheme of **HDMTDV**. ω is the frequency of the harmonic oscillator and Ω is the eigenfrequency of the numerical solution. h is the step size of the numerical integration. When $|\omega|h > 1.570792120\cdots$, Ω becomes occasionally complex , and the periodic nature of the numerical solution begins to break down.

When $\cos(2h\Omega)$ is real and the condition

$$|\cos(2h\Omega)| \leq 1\,, \tag{25}$$

is satisfied, the numerical solution given by the above discretization scheme becomes periodic with the correct amplitude (= 1). The relation given by Eq.(24) is shown in Fig.3 when ωh is real. This figure shows that the largest step size h_{max} which guarantees the purely periodic solution of Eq.(22) is given by

$$\begin{aligned} h_{max}|\omega| &= 1.57079212078280060208152\cdots \\ &= \frac{\pi}{2}(1 - 2.67763\cdots \times 10^{-6})\,. \end{aligned} \tag{26}$$

In other words, the largest step size which guarantees the periodic solution of Eq.(22) is 1/4 of the period of oscillation, and the relative error for the period is $2.67763\cdots\times 10^{-6}$. The local error of the discretization scheme becomes

$$\cos(2h\Omega) - \cos(2h\omega) = -\frac{(h\omega)^{12}}{20,956,320} + \cdots . \tag{27}$$

This analysis leads to the following conclusion. When we adopt the time step h as 1/20 of 1 period ($h = 0.1\pi/\omega$), the local error for function value is of the order of 4.4×10^{-14} and the error for the period of the solution is of the order of 1.1×10^{-13}. Furthermore, this discretization scheme can be proved to be linearly symplectic.

2.2. Difference Scheme for Variables with First Derivatives

In previous subsection, we have derived a discretization scheme for functions with second derivatives. Here, we consider the difference scheme for variables with no second order derivative, which appear in the equation like

$$0 = L\Big(\varphi(x),\ \varphi'(x),\ \psi(x),\ \psi'(x),\ \psi''(x),\ x\Big) . \tag{28}$$

In this case, the value $\varphi'(0)$ in Fig.2 cannot be specified as initial values. Then additional equations become needed if we use the discretization scheme in the preceding subsection. Sometimes, this process becomes a nuisance. We introduce therefore a separate discretization scheme for this case as shown in Fig.4.

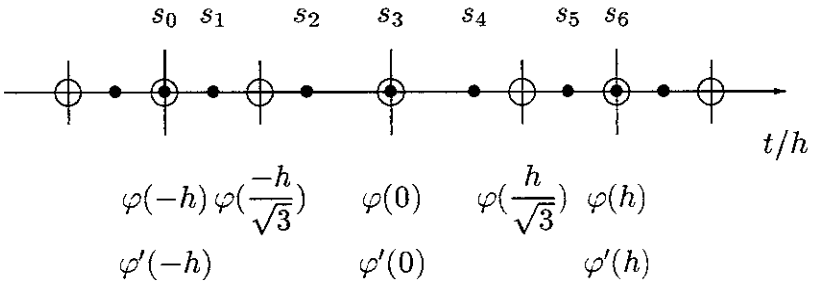

Fig.4 The difference scheme for variables having first derivatives (without second derivative) in Eq.(1), which should be solved at 7 points ($x = s_i h\ ,\quad i = 0,\ \cdots,\ 6$), shown by • (unequally separated points). The value $\varphi(-h)$ is given as initial values for rank-1 ordinary differential equations. The remaining 7 function values at grid points shown by ○ are obtained numerically. The values $s_i (i = 1, 2, 4, 5)$ are uniquely determined by the difference scheme for the variables with second derivative as shown in Eq.(5). The additional embedded points $x = \pm h/\sqrt{3}$ are determined from the condition that the truncation error for $\varphi'(s_i h)$ $(i = 1, 2, 4, 5)$ should be minimized.

Expressions of the function and its derivatives at the points $x = s_i h$ $(i = 0, \cdots, 6)$ are given by linear combinations of function values at grid points $x = \pm h,\ \pm hu,\ 0$ as follows

$$\varphi'(sh) = \frac{1}{h}\left(\sum_{j=-1}^{1} d_j(s)\varphi(jh) + f_-(s)\varphi(-hu) + f_+(s)\varphi(hu)\right) + \sum_{j=-1}^{1} e_j(s)\varphi'(jh), \tag{29}$$

$$\varphi(sh) = \sum_{j=-1}^{1} a_j(s)\varphi(jh) + c_-(s)\varphi(-hu) + c_+(s)\varphi(hu) + h\sum_{j=-1}^{1} b_j(s)\varphi'(jh)\,. \tag{30}$$

The difference scheme for the first derivative φ', Eq.(29), has a total of 8 parameters ($d_j(s)$, $e_j(s)$, $f_\pm(s)$). Then the truncation errors for Eq.(29) become $O(h^7)$. To reduce this truncation error one more order, we choose the value of the embedded points $h\,u$ appropriately. It is slightly surprising that the value $u = 1/\sqrt{3}$ guarantee the all truncation errors for $\varphi'(s_i h)$ $(i = 1, 2, 4, 5)$ are reduced one order, and the truncations errors of above expressions become $O(h^8)$ which is just the same order for discretization scheme of functions with second derivative shown in previous subsections. Coefficients for this discretization are reduced to the form

$$a_{\pm 1}(s) = \frac{293 + 85\Delta \pm (318 + 94\Delta)s}{3072}, \quad a_0(s) = \frac{61 - 19\Delta}{384}\,, \tag{31}$$

$$c_\pm(s) = \frac{3(111 - \Delta)(1 \pm s\sqrt{3})}{1024}\,, \tag{32}$$

$$b_{\pm 1}(s) = \frac{(25 + 9\Delta)(\mp - s)}{3072}, \quad b_0(s) = \frac{(61 - 19\Delta)s}{384}\,, \tag{33}$$

$$d_{\pm 1}(s) = \frac{\pm(1137 + 225\Delta) + (1380 + 292\Delta)s}{1536}, \quad d_0(s) = -\frac{(147 - 29\Delta)s}{48}\,, \tag{34}$$

$$f_\pm(s) = \frac{\mp(39 + 55\Delta)3\sqrt{3} + (216 - 168\Delta)3s}{1024}\,, \tag{35}$$

$$e_{\pm 1}(s) = \frac{-143 - 31\Delta \mp (168 + 40\Delta)s}{3072}, \quad e_0(s) = \frac{(-61 + 19\Delta)}{384}\,. \tag{36}$$

where the value Δ is given by Eq.(18).

We study the stability of the discretization scheme given by Eq.(31 –36) using the equation

$$\varphi'(x) = \lambda\varphi(x), \quad \varphi(0) = 1\,, \tag{37}$$

where λ is a some constant. The difference scheme Eq.(31–36) gives the following solution

$$\varphi(2h) = \frac{7560 + 7560\lambda h + 3465(\lambda h)^2 + 945(\lambda h)^3 + 165(\lambda h)^4 + 18(\lambda h)^5 + (\lambda h)^6}{7560 - 7560\lambda h + 3465(\lambda h)^2 - 945(\lambda h)^3 + 165(\lambda h)^4 - 18(\lambda h)^5 + (\lambda h)^6}\,. \tag{38}$$

This solution (the amplification factor of the difference scheme) has the following characteristics

$$|\varphi(2h)| < 1 \quad \text{when } \Re\,\lambda h < 0\ , \tag{39}$$

$$|\varphi(2h)| = 1 \quad \text{when } \lambda h \text{ is pure imaginary.} \tag{40}$$

The relation (39) shows that the difference scheme is A-stable and Eq.(40) guarantees purely periodic numerical solutions independent of the step size h when λ is pure imaginary. The linear symplectic nature is also verified for this discretization scheme. The local error of the difference scheme is given by the difference between the discretized solution Eq.(38) and the analytic solution $\exp(2\lambda h)$

$$\varphi(2h) - \exp(2\lambda h) = -\frac{(\lambda h)^{11}}{13,097,700} + \cdots\ . \tag{41}$$

These results show the excellent nature of the difference scheme of Eq.(31–36).

2.3. Difference Scheme for Variables with no Derivatives

Here, we consider the difference scheme for the variables with no derivatives, which appear in the equation like

$$0 = L\Big(\varphi(x),\ \psi(x),\ \psi'(x),\ \xi(x),\ \xi'(x),\ \xi''(x),\ x\Big)\ . \tag{42}$$

In this case the difference scheme is very simple, as shown in Fig.5, and and no truncation errors are included.

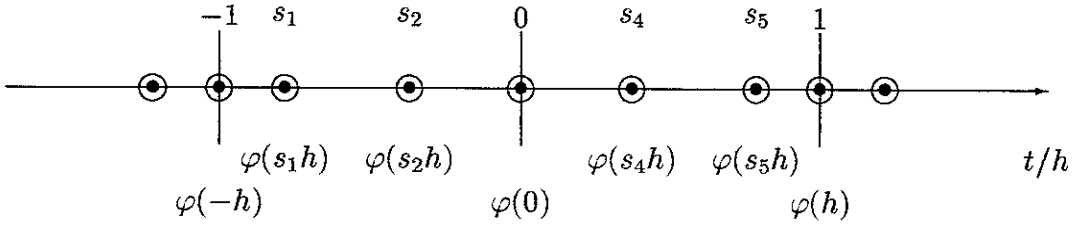

Fig.5 The difference scheme for variables having no derivatives in Eq.(1), which should be solved at a total of 7 points ($x = s_ih,\ i = 0,\cdots,6$), shown by • (unequally separated points). The values $\varphi(s_ih)$ ($i = 0,1,\cdots,6$) shown by ○ are obtained numerically. The values $s_i (i = 1,2,4,5)$ are uniquely determined by the difference scheme for the variables with second derivative as shown in Eq.(5). ($s_0 = -1,\ s_3 = 0,\ s_6 = 1$)

2.4. Remarks on the coding of the program

In previous sections, we have considered the truncation error of the discretization method. In actual numerical computations the roundoff errors deteriorate the accuracy of derivatives. To reduce these effects, increments of variables are treated as

practical unknown quantities in the actual program coding. For example, the quantities $\tilde{\varphi}(jh)$ $\tilde{\varphi}'(jh)$ are treated as unknown quantities introduced by the relations

$$\varphi(jh) = \varphi(-h) + (j+1)h\varphi'(-h) + \tilde{\varphi}(jh) \ , \tag{43}$$

$$\varphi'(jh) = \varphi'(-h) + \tilde{\varphi}'(jh) \ , \tag{44}$$

$$(j = 0, 1) \ .$$

If it is possible to determine all the highest derivatives using the given system of equation (1), we can get solutions directly by the above mentioned algorithm. There are, however, problems in which we cannot determine the highest derivatives only by the given system of equations. An example is given by

$$G\Big(\varphi'', \psi'', \varphi, \psi, x\Big) = 0 \ , \tag{45}$$

$$H\Big(\varphi, \psi, x\Big) = 0 \ . \tag{46}$$

In this case, both variables $\varphi(x)$, $\psi(x)$ have second derivatives, so the discretization scheme given by Eq.(9 –17) is applied. This discretization scheme assumes that $\varphi(-h)$, $\varphi'(-h)$, $\psi(-h)$ and $\psi'(-h)$ are given as initial conditions. In this example, however, we have only two true initial conditions, for example $\varphi(-h)$ and $\varphi'(-h)$. The other quantities $\psi(-h)$ and $\psi'(-h)$ are not initial conditions, and should be determined consistently from Eq.(46). In this case, two additional equations are necessary to determine the values $\psi(-h)$ and $\psi'(-h)$. An example of a set of additional equations is

$$\frac{d}{dx} H\Big(\varphi, \psi, x\Big) = 0 \ , \tag{47}$$

$$\frac{d^2}{dx^2} H\Big(\varphi, \psi, x\Big) = 0 \ . \tag{48}$$

Since the program should be informed of these facts, a index for each variables is prepared in the program. Example of the index is rank-2 array variable named JVR as shown in the following.

$JVR(1,n)$ = highest derivatives of n-th variable.
$JVR(2,n)$ = number of additional equations for n-th variable.

When equation is one of standard form as

$$\varphi'' = f(\varphi', \varphi, x) \ , \tag{49}$$

and high speed computations is requested, separate program should be prepared which does not treat the second variables as unknown functions because this value is given

in Eq.(49) . In this case the computation speed can exceed the speed of standard Runge-Kutta method program.

3. Numerical Examples of HDMTDV

In this section we show several numerical examples of **HDMTDV**. Computation was carried out on a Fujitsu M-1800 with double precision (1 word is 64 bits). The 'exact value' is calculated by long double accuracy (1 word is 128 bits). First we show the accuracy of the discretization scheme of **HDMTDV**. Giving the 'exact values' of $\varphi(nh)$, $\varphi'(nh)$, $\varphi''(nh)$ on each grid points ($\varphi(x) = \sin(x)$, n =integer and $h = \pi/32$), we have calculated the numerical error of the discretization scheme given by Eqs.(9–17) and plotted it in Fig.6.

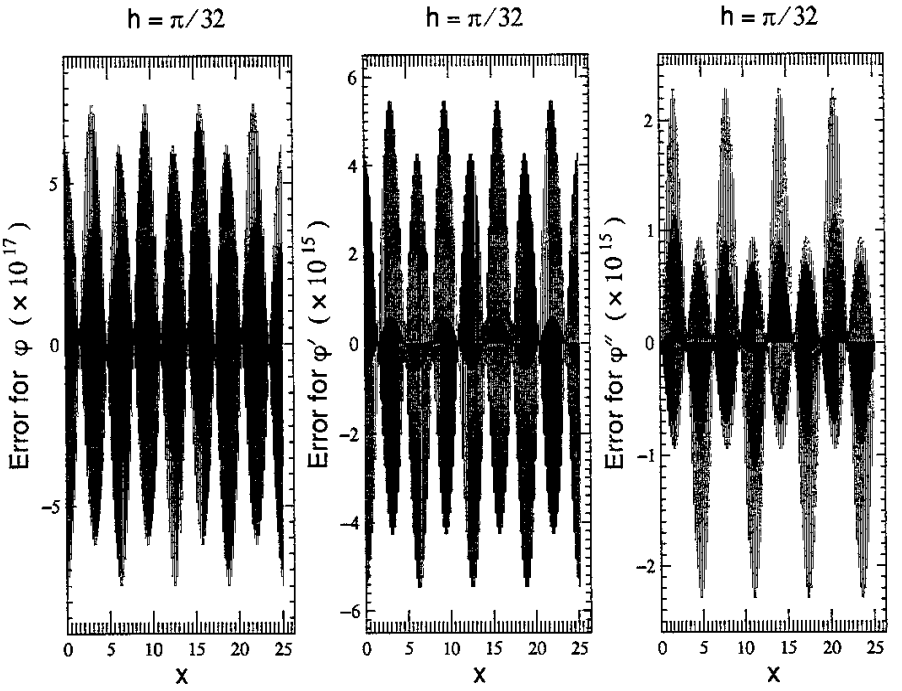

Fig.6 An example of numerical error of the discretization scheme given by Eqs.(9–17). First and second derivatives (φ' and φ'') have almost the same order of accuracy and the accuracy for φ is one order higher compared to them.

Next, we have calculated the numerical error for the variables with first order derivative (without second order derivative). The discretization scheme is given by Eqs.(31–36). In this case, we give the 'exact values' of $\varphi(nh)$ and $\varphi'(nh)$ on each grid points and $\varphi((2n+1\pm 1/\sqrt{3})h)$ on embedded points ($\varphi(x) = \sin(x)$, n =integer and $h = \pi/32$), and calculate $\varphi((2n+1+s_i)h)$ and $\varphi'((2n+1+s_i)h)$ by the discretization

scheme Eqs.(31–36). The numerical error for this discretization scheme is shown in Fig.7.

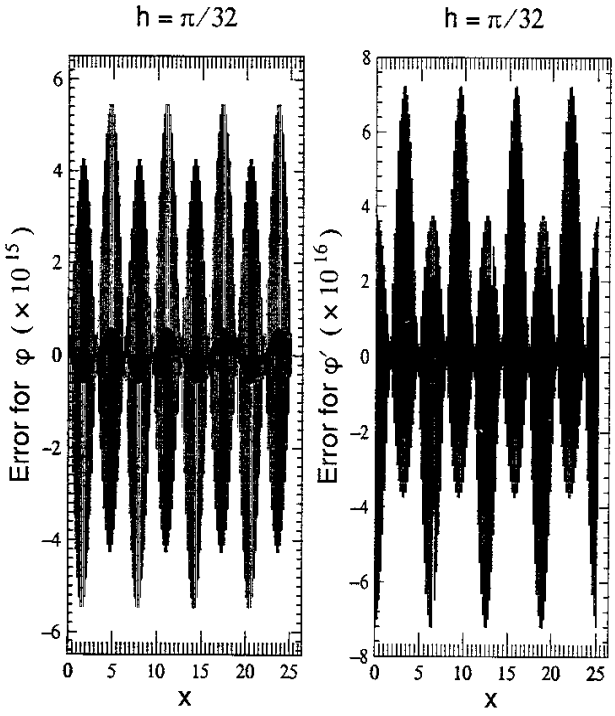

Fig.7 An example of numerical error of the discretization scheme given by Eqs.(31–36). φ and φ' have almost the same order of accuracy.

3.1. Kepler Motion

As a example of dissipationless dynamical systems, we have integrated the equation for the Kepler motion

$$\frac{d^2x}{dt^2} = -\mu\frac{x}{(x^2+y^2)^{3/2}}\,, \tag{50}$$

$$\frac{d^2y}{dt^2} = -\mu\frac{y}{(x^2+y^2)^{3/2}}\,, \tag{51}$$

$$\mu = \pi^2/16\,,$$

$$x(0) = \frac{3}{4}\,, \quad \frac{dx(0)}{dt} = 0\,,$$

$$y(0) = 0\,, \quad \frac{dy(0)}{dt} = \pi\sqrt{\frac{29}{192}}\,,$$

where the constant μ and the initial conditions are chosen such that the analytic solution has period $T = 64$ and a relatively large value for the eccentricity. In this system energy and angular momentum are conserved and it is possible to check the accuracy of the numerical computations.

For this system the index of the variables is shown in Table 1. No additional equations are necessary.

variables	$x(t)$	$y(t)$
n	1	2
$JVR(1,n)$	2	2
$JVR(2,n)$	0	0

Table 1 Index JVR of each variables to solve the Kepler motion given by Eqs.(50–51) by **HDMTDV**.

For the numerical computations by **HDMTDV**, we have used step size $h = 0.25(= T/256)$ and total time step number 10^6 ($0 \leq t \leq 5 \times 10^5$). Plots of the orbit $(x(t), y(t))$ and of the error for energy and angular momentum are shown in Fig.8 and Fig.9.

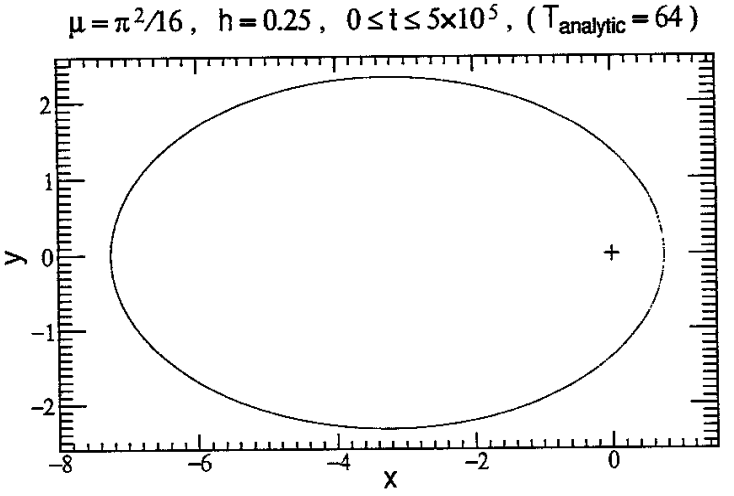

Fig.8 Plot of the orbit $(x(t), y(t))$ of the Kepler motion Eq.(50–51). Because the period for the numerical solution is not the same of the analytical one (= 64), the phase of the motion gradually shifts from the analytical position. The discrete plots of $(x(t), y(t))$ appears like a continuous line. But the motion is guaranteed to come back to the initial state. No secular error are present in the numerical results. The center of the force is marked by '+'.

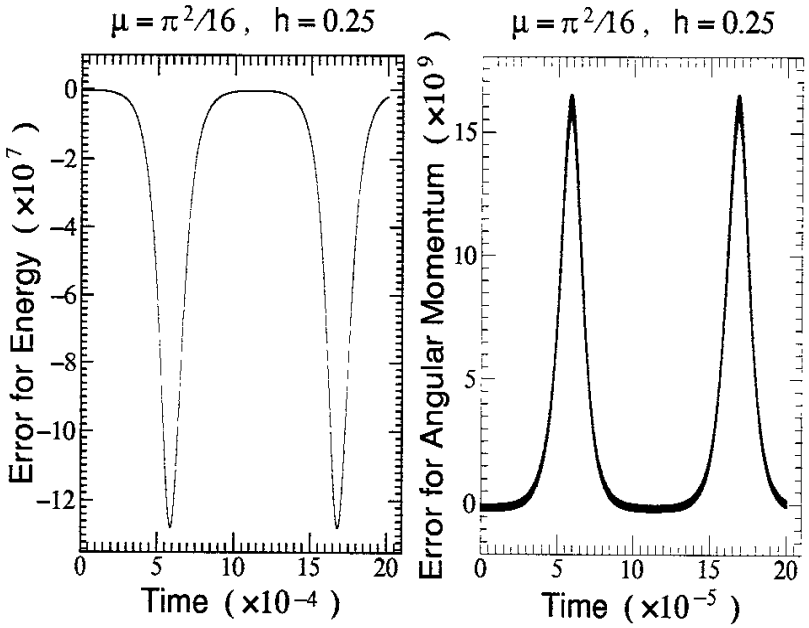

Fig.9 Plot of error for energy and angular momentum of the numerical solution of Eq.(50–51) (Kepler Motion). Because the period of the numerical solution is very close to the analytical value (= 64), the recursion time of the numerical solution is very long. This figure shows the secular error free computation characteristics of **HDMTDV**.

3.2. Numerical Solution of a Connected Rigid Pendulum

In this section we solve the motion of a connected rigid body pendulum as an example of differential-algebraic equations. The equations are

$$m_1\left(\frac{d^2x_1}{dt^2}-g\right)=-T_1\cdot x_1+T_2\cdot(x_2-x_1)\,, \tag{52}$$

$$m_1\frac{d^2y_1}{dt^2}=-T_1\cdot y_1+T_2\cdot(y_2-y_1)\,, \tag{53}$$

$$m_2\left(\frac{d^2x_2}{dt^2}-g\right)=-T_2\cdot(x_2-x_1)\,, \tag{54}$$

$$m_2\frac{d^2y_2}{dt^2}=-T_2\cdot(y_2-y_1)\,, \tag{55}$$

$$\sqrt{x_1^2+y_1^2}=\ell_1\,, \tag{56}$$

$$\sqrt{(x_1-x_2)^2+(y_1-y_2)^2}=\ell_2\,, \tag{57}$$

where ℓ_1 and ℓ_2 represent the length of mass-less rigid rods. T_1 and T_2 correspond to to the tensions of the rigid rods, m_1, m_2, g are constants. The unknown variables are the position of the tip of each rod (x_1, y_1, x_2, y_2) and the tension of each rod, (T_1 and T_2). The former group of variables has second derivatives, but last group of variables has no derivatives. In this case, the the index JVR is given in Table 2.

variables	x_1	y_1	x_2	y_2	T_1	T_2
n	1	2	3	4	5	6
$JVR(1,n)$	2	2	2	2	0	0
$JVR(2,n)$	0	2	0	2	0	0

Table 2 Index JVR of each variables to solve the differential-algebraic equations given by Eqs.(52– 57) by **HDMTDV**.

The system of Eqs.(52–57) has energy conservation law given by

$$\begin{aligned} E &\equiv \sum_{i=1}^{2} \frac{m_i}{2} \left[\left(\frac{d\,x_i}{d\,t} \right)^2 + \left(\frac{d\,y_i}{d\,t} \right)^2 \right] - m_i g x_i \\ &= \text{constant}, \end{aligned} \tag{58}$$

which is used to check the accuracy of the numerical results.

Numerical example are shown in Figs.10 and 11.

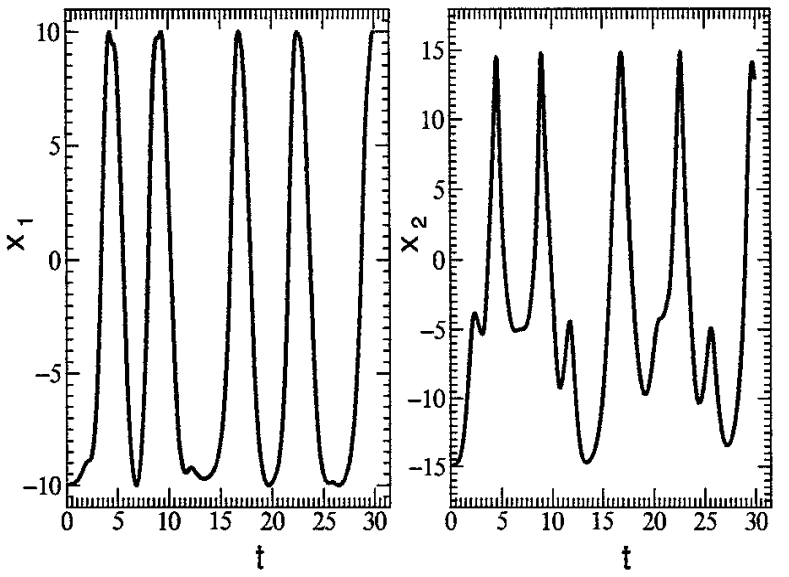

Fig.10 Numerical solution of Eq.(52–57) by **HDMTDV** with step size $h = 0.001$. x_1 and x_2 are plotted as a function of time. $m_1 = 65$, $m_2 = 35$, $\ell_1 = 10$, $\ell_2 = 5$, $g = 9.8$. Initial angle of rod-1= 175 (deg), rod-2= 187 (deg). Initial velocities of rods are assumed to be 0.

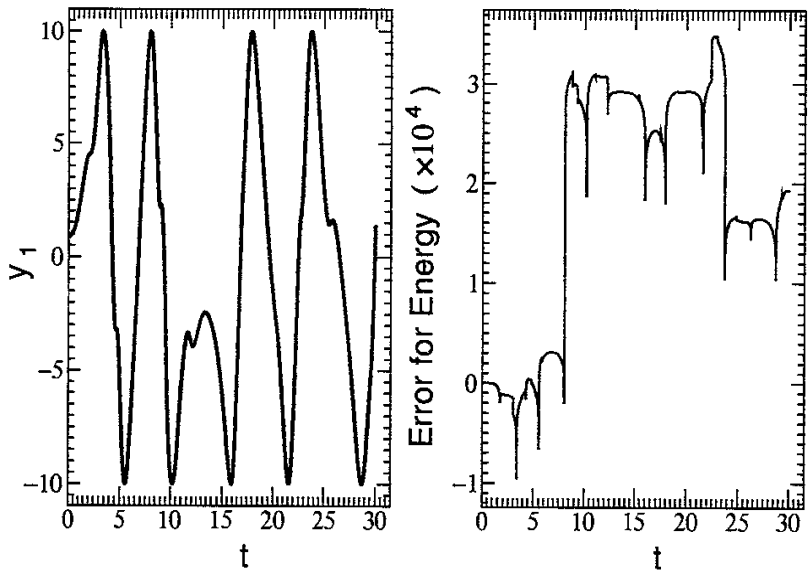

Fig.11 Numerical solution of Eq.(52-57) by **HDMTDV** with step size $h = 0.001$. y_1 and the error for the energy are plotted as a function of time. Parameters and initial conditions are the same of those of Fig.10.

This system is dissipationless, but numerical results show that numerical error suddenly increase at special points. This will break the time reversal nature of the motion. The reason of this phenomena will be discussed in the next section.

3.3. Differential-Algebraic Equation of Index 2

As an example of differential-algebraic equation of index 2, we have integrated the following equations by **HDMTDV**,

$$0 = L_1(y, y', z, t) \equiv \frac{dy}{dt} - \alpha\cos(t)z^2 - \beta\exp(-t)y^2 , \tag{59}$$

$$0 = L_2(y, t) \equiv 1 - \Big(1 - \alpha\sin(t) + \beta\exp(-t)\Big) \cdot y , \tag{60}$$

where α and β are constants. The analytical solution of this system is given by

$$y(t) = z(t) = \frac{1}{1 - \alpha\sin(t) + \beta\exp(-t)} . \tag{61}$$

In this case the variable $y(t)$ contains the first order derivative, but it is determined by the algebraic Eq.(60). Then, an additional equation is necessary to determine the value $y'(t)$. So, the index of the variables $y(t)$ and $z(t)$ becomes as shown in Table 3.

variables	$y(t)$	$z(t)$
n	1	2
$JVR(1,n)$	1	0
$JVR(2,n)$	1	0

Table 3 Index JVR of each variables to solve the differential-algebraic equations of index-2 given by Eqs.(59–60) by **HDMTDV**.

We adopted as additional equation

$$\left.\frac{d\,L_2(y,t)}{d\,t}\right|_{t=(2n-1)h} = 0\,. \quad n : \text{positive integer.} \tag{62}$$

Numerical results of **HDMTDV** for this differential-algebraic equations are shown in Fig.12.

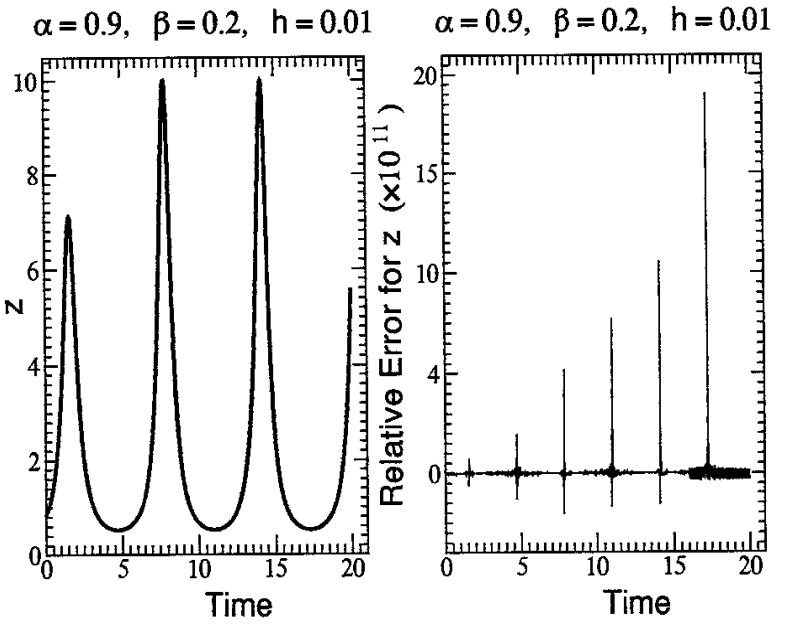

Fig.12 Plot of numerical solution and its relative error for differential-algebraic equations of index-2, Eq.(59–60). Since the variables $z(t)$ is solved by the algebraic equation, Eq.(60), the error is only due to roundoff error, i.e., order of 10^{-15}.

4. Summary and Discussion

We have developed a new integration method with high accuracy and high applicability. A new program named **HDMTDV** can solve dissipationless dynamical

systems without secular error. Stiff ordinary equations or differential-algebraic equations can also be solved by the same program. These properties are demonstrated by several numerical examples.

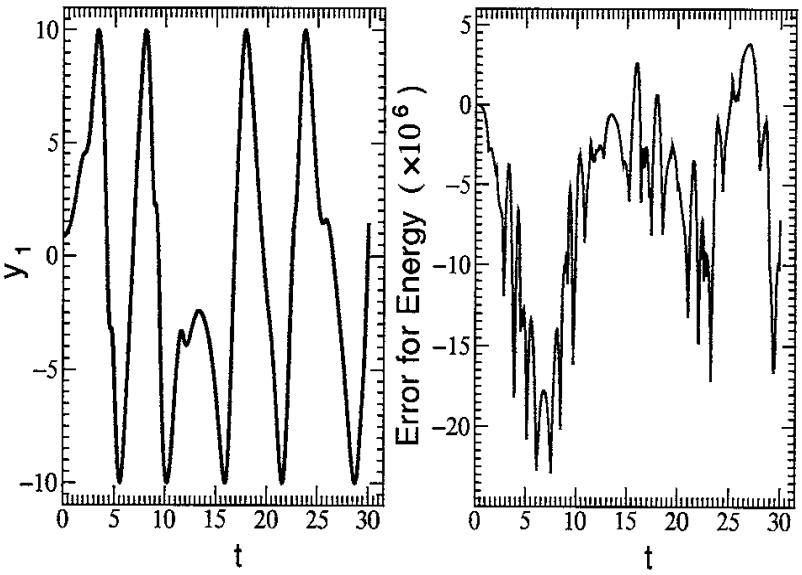

Fig.13 Numerical solution of Eq.(52–57) by **HDMTDV** under automatic change of the value of JVR guided by the Table 4. y_1 and the error for the energy are plotted as a function of time. Parameters and initial conditions are the same of those of Fig.10.

In subsection 3.2, we have observed a sudden increase of numerical errors. Let us consider the reason of this phenomena. When we treat the constraint given by Eq.(56), we use two additional equations,

$$x_1 x_1' + y_1 y_1' = 0\,, \tag{63}$$

$$x_1 x_1'' + x_1' x_1' + y_1 y_1'' + y_1' y_1' = 0\,. \tag{64}$$

These equations are expected to work to determine the values $y'(t)$ and $y''(t)$. But, when the rod is nearly vertical ($x_1 \simeq \ell_1$ and $y_1 \simeq 0$), the left hand side of Eqs.(63–64) becomes very close to zero independently of the values of $y'(t)$ and $y''(t)$, and it becomes difficult to determine the accurate value of $y'(t)$ and $y''(t)$. This will be the reason of the sudden increase of numerical errors shown in Fig.11.

A quick treatment for this problem is provided by the replacement of the value of the index JVR according to the relation $|y_1| \geq |x_1|$ or $|y_1| < |x_1|$, i.e., in the former case, we treat $y_1(t)$ as a rank-2 variable, on the other hand, in the latter case, we treat $x_1(t)$ as a rank-2 variable as shown in the Table 4.

		$\|y_1\| \geq \|x_1\|$		$\|y_1\| < \|x_1\|$	
variables	n	$JVR(1,n)$	$JVR(2,n)$	$JVR(1,n)$	$JVR(2,n)$
x_1	1	2	0	2	2
y_1	2	2	2	2	0

		$\|y_2 - y_1\| \geq \|x_2 - x_1\|$		$\|y_2 - y_1\| < \|x_2 - x_1\|$	
variables	n	$JVR(1,n)$	$JVR(2,n)$	$JVR(1,n)$	$JVR(2,n)$
x_2	3	2	0	2	2
y_2	4	2	2	2	0

Table 4 An improved index JVR to solve the differential-algebraic equations given by Eqs.(52– 57) by **HDMTDV**. The index JVR for the values T_1 and T_2 are same of those of Table 2.

The physical meaning of this process is the following. We treat $y_1(t)$ as a rank-2 variable when $|y_1(t)| \geq |x_1(t)|$. In this case, $y_1'(-h)$ is treated as a initial condition and $y_1''(-h)$ is determined by the equation of motions. The $x_1'(-h)$ and $x_1''(-h)$ are determined by the additional equations Eqs.(63–64). When $|y_1(t)| > |x_1(t)|$, $x_1(t)$ is treated as a rank-2 variables. We show a numerical example in Fig.13, using this choice of the value of the index JVR.

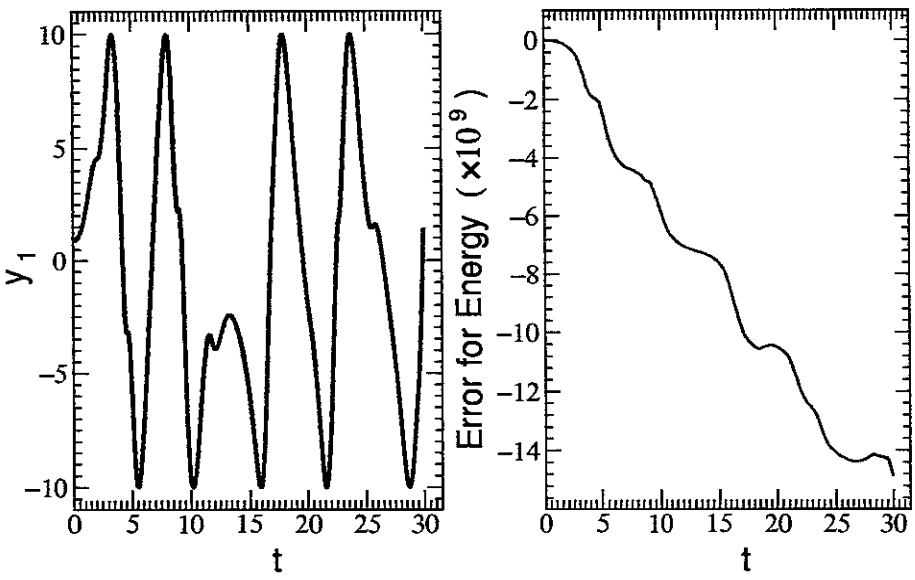

Fig.14 Numerical solution of Eq.(52–57) by **HDMTDV** introducing the polar angles θ_1 and θ_2 defined in Eqs.(65–66). y_1 and the error for the energy are plotted as a function of time. Parameters and initial conditions are the same of those of Fig.10.

A more fundamental treatment for this problems is the introduction of polar angles, θ_1 and θ_2 as unknown variables instead of x_1, y_1, x_2 and y_2,

$$x_1 = \ell_1 \cos\theta_1 \ , \qquad y_1 = \ell_1 \sin\theta_1 \ , \tag{65}$$

$$x_2 - x_1 = \ell_2 \cos\theta_2 \ , \qquad y_2 - y_1 = \ell_2 \sin\theta_2 \ . \tag{66}$$

In this case, Eqs.(56–57) are automatically satisfied. Highly accurate numerical solution is obtained as shown in Fig.14.

In subsection 2.1, we found that two of the coefficients $(A_j(s_i),\ B_j(s_i),\ C_j(s_i))$. $(j = -1, 0, 1,\ i = 0, \cdots, 6)$ are undetermined (for example the values of $C_1(s_4$ and $C_1(s_5)$, if we are satisfied with the compatibility for the truncation errors for representations Eqs.(2–3). In this case, we can change the dispersion relation Eq.(24) so as to satisfy

$$\cos(2h\Omega) \leq 1, \quad \text{for} \quad h|\omega| \lesssim \frac{3\pi}{2} \ , \tag{67}$$

by appropriate choice of the values of $C_1(s_4)$ and $C_1(s_5)$. In this case, the largest step size h_{max} which guarantees the purely periodic solution of Eq.(22) is given by 3/4 of the period of oscillation.

It will be easy to extend **HDMTDV** to solve boundary value and eigenvalue problems. This will be published elsewhere.

The next big task is the construction of a general purpose computer program to solve time evolution of multi-dimension boundary value problems described by partial differential equations. When the space dimension is 1-D, we have already constructed such a general purpose computer program based on **HIDM**[14,15]. The present work represents also an important contribution to accomplish this task.

5. Acknowledgements

G. Gnudi acknowledges the *Japan Society for the Promotion of Science* for the financial support.

6. References

1. K. E. Brenan, *Annals of Numerical Mathematics*, **1** (1994) 247.
2. S. L. Campbell, *Annals of Numerical Mathematics*, **1** (1994) 265.
3. R. März, *Annals of Numerical Mathematics*, **1** (1994) 279.
4. T. Watanabe, *Annals of Numerical Mathematics*, **1** (1994) 293.
5. K. Abe, A. Ishida, T. Watanabe, Y. Kanada and K. Nishikawa, *Kakuyugo Kenkyu* (In Japanese), **57** (1987) 85.
6. T. Watanabe and M. Takagi, *Trans. JPN Soc. Ind. and Appl. Mat.* (In Japanese), **1** (1991) 135.

7. T. Watanabe, K. Abe, A. Ishida, Y. Kanada and K. Nishikawa, *Kakuyugo Kenkyu* (In Japanese), **58** (1987) 265-278.
8. T. Watanabe, *RIMS koukyuuroku* (Research Institute for Mathematical Science, Kyoto University) (In Japanese), **841** (1993) 43.
9. J. M. Sanz-Serna, *BIT*, **28** (1988) 877.
10. S. Saito, H. Sugiura and T, Mitsui, *BIT*, **345** (1992) 345.
11. H. Yoshida, *Cel. Mech. and Dyn. Astr.*, **56** (1993) 27.
12. G. Gnudi and T. Watanabe, *J. Phys. Soc. JPN*, **62** (1993) 3492.
13. T. Watanabe and G. Gnudi, *ISM Cooperative Research Report* (In Japanese), **55** (1994) 211.
14. T. Watanabe, *Trans. JPN Soc. Ind. and Appl. Mat.* (In Japanese), **2** (1992) 93.
15. T. Watanabe, *GAKUTO International Series, Mathematical Science and Applications*, **1** (1993) 189.

Recent Issues of NIFS Series

NIFS-299 K. Toi, T. Morisaki, S. Sakakibara, A. Ejiri, H. Yamada, S. Morita, K. Tanaka, N. Nakajima, S. Okamura, H. Iguchi, K. Ida, K. Tsumori, S. Ohdachi, K. Nishimura, K. Matsuoka, J. Xu, I. Yamada, T. Minami, K. Narihara, R. Akiyama, A. Ando, H. Arimoto, A. Fujisawa, M. Fujiwara, H. Idei, O. Kaneko, K. Kawahata, A. Komori, S. Kubo, R. Kumazawa, T. Ozaki, A. Sagara, C. Takahashi, Y. Takita and T. Watari,
Impact of Rotational-Transform Profile Control on Plasma Confinement and Stability in CHS; Aug. 1994 (IAEA-CN-60/A6/C-P-3)

NIFS-300 H. Sugama and W. Horton,
Dynamical Model of Pressure-Gradient-Driven Turbulence and Shear Flow Generation in L-H Transition; Aug. 1994 (IAEA/CN-60/D-P-I-11)

NIFS-301 Y. Hamada, A. Nishizawa, Y. Kawasumi, K.N. Sato, H. Sakakita, R. Liang, K. Kawahata, A. Ejiri, K. Narihara, K. Sato, T. Seki, K. Toi, K. Itoh, H. Iguchi, A. Fujisawa, K. Adachi, S. Hidekuma, S. Hirokura, K. Ida, M. Kojima, J. Koog, R. Kumazawa, H. Kuramoto, T. Minami, I. Negi, S. Ohdachi, M. Sasao, T. Tsuzuki, J. Xu, I. Yamada, T. Watari,
Study of Turbulence and Plasma Potential in JIPP T-IIU Tokamak; Aug. 1994 (IAEA/CN-60/A-2-III-5)

NIFS-302 K. Nishimura, R. Kumazawa, T. Mutoh, T. Watari, T. Seki, A. Ando, S. Masuda, F. Shinpo, S. Murakami, S. Okamura, H. Yamada, K. Matsuoka, S. Morita, T. Ozaki, K. Ida, H. Iguchi, I. Yamada, A. Ejiri, H. Idei, S. Muto, K. Tanaka, J. Xu, R. Akiyama, H. Arimoto, M. Isobe, M. Iwase, O. Kaneko, S. Kubo, T. Kawamoto, A. Lazaros, T. Morisaki, S. Sakakibara, Y. Takita, C. Takahashi and K. Tsumori,
ICRF Heating in CHS; Sep. 1994 (IAEA-CN-60/A-6-I-4)

NIFS-303 S. Okamura, K. Matsuoka, K. Nishimura, K. Tsumori, R. Akiyama, S. Sakakibara, H. Yamada, S. Morita, T. Morisaki, N. Nakajima, K. Tanaka, J. Xu, K. Ida, H. Iguchi, A. Lazaros, T. Ozaki, H. Arimoto, A. Ejiri, M. Fujiwara, H. Idei, A. Iiyoshi, O, Kaneko, K. Kawahata, T. Kawamoto, S. Kubo, T. Kuroda, O. Motojima, V.D. Pustovitov, A. Sagara, C. Takahashi, K. Toi and I. Yamada,
High Beta Experiments in CHS; Sep. 1994 (IAEA-CN-60/A-2-IV-3)

NIFS-304 K. Ida, H. Idei, H. Sanuki, K. Itoh, J. Xu, S. Hidekuma, K. Kondo, A. Sahara, H. Zushi, S.-I. Itoh, A. Fukuyama, K. Adati, R. Akiyama, S. Bessho, A. Ejiri, A. Fujisawa, M. Fujiwara, Y. Hamada, S. Hirokura, H. Iguchi, O. Kaneko, K. Kawahata, Y. Kawasumi, M. Kojima, S. Kubo, H. Kuramoto, A. Lazaros, R. Liang, K. Matsuoka, T. Minami, T. Mizuuchi, T. Morisaki, S. Morita, K. Nagasaki, K. Narihara, K. Nishimura, A. Nishizawa, T. Obiki, H. Okada, S. Okamura, T. Ozaki, S. Sakakibara, H. Sakakita, A. Sagara, F. Sano, M. Sasao, K. Sato, K.N. Sato, T. Saeki, S. Sudo, C. Takahashi, K. Tanaka, K. Tsumori, H.Yamada, I. Yamada, Y. Takita, T. Tuzuki, K. Toi and T. Watari,

Control of Radial Electric Field in Torus Plasma; Sep. 1994
(IAEA-CN-60/A-2-IV-2)

NIFS-305 T. Hayashi, T. Sato, N. Nakajima, K. Ichiguchi, P. Merkel, J. Nührenberg, U. Schwenn, H. Gardner, A. Bhattacharjee and C.C.Hegna,
Behavior of Magnetic Islands in 3D MHD Equilibria of Helical Devices;
Sep. 1994 (IAEA-CN-60/D-2-II-4)

NIFS-306 S. Murakami, M. Okamoto, N. Nakajima, K.Y. Watanabe, T. Watari, T. Mutoh, R. Kumazawa and T. Seki,
Monte Carlo Simulation for ICRF Heating in Heliotron/Torsatrons;
Sep. 1994 (IAEA-CN-60/D-P-I-14)

NIFS-307 Y. Takeiri, A. Ando, O. Kaneko, Y. Oka, K. Tsumori, R. Akiyama, E. Asano, T. Kawamoto, T. Kuroda, M. Tanaka and H. Kawakami,
Development of an Intense Negative Hydrogen Ion Source with a Wide-Range of External Magnetic Filter Field; Sep. 1994

NIFS-308 T. Hayashi, T. Sato, H.J. Gardner and J.D. Meiss,
Evolution of Magnetic Islands in a Heliac; Sep. 1994

NIFS-309 H. Amo, T. Sato and A. Kageyama,
Intermittent Energy Bursts and Recurrent Topological Change of a Twisting Magnetic Flux Tube; Sep.1994

NIFS-310 T. Yamagishi and H. Sanuki,
Effect of Anomalous Plasma Transport on Radial Electric Field in Torsatron/Heliotron; Sep. 1994

NIFS-311 K. Watanabe, T. Sato and Y. Nakayama,
Current-profile Flattening and Hot Core Shift due to the Nonlinear Development of Resistive Kink Mode; Oct. 1994

NIFS-312 M. Salimullah, B. Dasgupta, K. Watanabe and T. Sato,
Modification and Damping of Alfvén Waves in a Magnetized Dusty Plasma; Oct. 1994

NIFS-313 K. Ida, Y. Miura, S -I. Itoh, J.V. Hofmann, A. Fukuyama, S. Hidekuma, H. Sanuki, H. Idei, H. Yamada, H. Iguchi, K. Itoh,
Physical Mechanism Determining the Radial Electric Field and its Radial Structure in a Toroidal Plasma; Oct. 1994

NIFS-314 Shao-ping Zhu, R. Horiuchi, T. Sato and The Complexity Simulation Group,
Non-Taylor Magnetohydrodynamic Self-Organization; Oct. 1994

NIFS-315 M. Tanaka,
Collisionless Magnetic Reconnection Associated with Coalescence of

Flux Bundles; Nov. 1994

NIFS-316 M. Tanaka,
Macro-EM Particle Simulation Method and A Study of Collisionless Magnetic Reconnection; Nov. 1994

NIFS-317 A. Fujisawa, H. Iguchi, M. Sasao and Y. Hamada,
Second Order Focusing Property of 210° Cylindrical Energy Analyzer; Nov. 1994

NIFS-318 T. Sato and Complexity Simulation Group,
Complexity in Plasma - A Grand View of Self- Organization; Nov. 1994

NIFS-319 Y. Todo, T. Sato, K. Watanabe, T.H. Watanabe and R. Horiuchi,
MHD-Vlasov Simulation of the Toroidal Alfvén Eigenmode; Nov. 1994

NIFS-320 A. Kageyama, T. Sato and The Complexity Simulation Group,
Computer Simulation of a Magnetohydrodynamic Dynamo II: Nov. 1994

NIFS-321 A. Bhattacharjee, T. Hayashi, C.C.Hegna, N. Nakajima and T. Sato,
Theory of Pressure-induced Islands and Self-healing in Three-dimensional Toroidal Magnetohydrodynamic Equilibria; Nov. 1994

NIFS-322 A. Iiyoshi, K. Yamazaki and the LHD Group,
Recent Studies of the Large Helical Device; Nov. 1994

NIFS-323 A. Iiyoshi and K. Yamazaki,
The Next Large Helical Devices; Nov. 1994

NIFS-324 V.D. Pustovitov
Quasisymmetry Equations for Conventional Stellarators; Nov. 1994

NIFS-325 A. Taniike, M. Sasao, Y. Hamada, J. Fujita, M. Wada,
The Energy Broadening Resulting from Electron Stripping Process of a Low Energy Au^- Beam; Dec. 1994

NIFS-326 I. Viniar and S. Sudo,
New Pellet Production and Acceleration Technologies for High Speed Pellet Injection System "HIPEL" in Large Helical Device; Dec. 1994

NIFS-327 Y. Hamada, A. Nishizawa, Y. Kawasumi, K. Kawahata, K. Itoh, A. Ejiri, K. Toi, K. Narihara, K. Sato, T. Seki, H. Iguchi, A. Fujisawa, K. Adachi, S. Hidekuma, S. Hirokura, K. Ida, M. Kojima, J. Koong, R. Kumazawa, H. Kuramoto, R. Liang, T. Minami, H. Sakakita, M. Sasao, K.N. Sato, T. Tsuzuki, J. Xu, I. Yamada, T. Watari,
Fast Potential Change in Sawteeth in JIPP T-IIU Tokamak Plasmas; Dec. 1994

NIFS-328 V.D. Pustovitov,
Effect of Satellite Helical Harmonics on the Stellarator Configuration;

Dec. 1994

NIFS-329 K. Itoh, S-I. Itoh and A. Fukuyama,
A Model of Sawtooth Based on the Transport Catastrophe; Dec. 1994

NIFS-330 K. Nagasaki, A. Ejiri,
Launching Conditions for Electron Cyclotron Heating in a Sheared Magnetic Field; Jan. 1995

NIFS-331 T.H. Watanabe, Y. Todo, R. Horiuchi, K. Watanabe, T. Sato,
An Advanced Electrostatic Particle Simulation Algorithm for Implicit Time Integration; Jan. 1995

NIFS-332 N. Bekki and T. Karakisawa,
Bifurcations from Periodic Solution in a Simplified Model of Two-dimensional Magnetoconvection; Jan. 1995

NIFS-333 K. Itoh, S.-I. Itoh, M. Yagi, A. Fukuyama,
Theory of Anomalous Transport in Reverse Field Pinch; Jan. 1995

NIFS-334 K. Nagasaki, A. Isayama and A. Ejiri
Application of Grating Polarizer to 106.4GHz ECH System on Heliotron-E; Jan. 1995

NIFS-335 H. Takamaru, T. Sato, R. Horiuchi, K. Watanabe and Complexity Simulation Group,
A Self-Consistent Open Boundary Model for Particle Simulation in Plasmas; Feb. 1995

NIFS-336 B.B. Kadomtsev,
Quantum Telegragh : is it possible?; Feb. 1995

NIFS-337 B.B.Kadomtsev,
Ball Lightning as Self-Organization Phenomenon; Feb. 1995

NIFS-338 Y. Takeiri, A. Ando, O. Kaneko, Y. Oka, K. Tsumori, R. Akiyama, E. Asano, T. Kawamoto, M. Tanaka and T. Kuroda,
High-Energy Acceleration of an Intense Negative Ion Beam; Feb. 1995

NIFS-339 K. Toi, T. Morisaki, S. Sakakibara, S. Ohdachi, T.Minami, S. Morita, H. Yamada, K. Tanaka, K. Ida, S. Okamura, A. Ejiri, H. Iguchi, K. Nishimura, K. Matsuoka, A. Ando, J. Xu, I. Yamada, K. Narihara, R. Akiyama, H. Idei, S. Kubo, T. Ozaki, C. Takahashi, K. Tsumori,
H-Mode Study in CHS; Feb. 1995

NIFS-340 T. Okada and H. Tazawa,
Filamentation Instability in a Light Ion Beam-plasma System with External Magnetic Field; Feb. 1995